CO_2 INJECTION FOR GEOLOGICAL STORAGE

Ernestos Sarris[1], Elias Gravanis[2] and Panos Papanastasiou[3]

Department of Civil and Environmental Engineering

University of Cyprus

Nicosia 1678, Cyprus

[1]e-mail: esarris@ucy.ac.cy

[2] e-mail: eliasgravanis@hotmail.com

[3]e-mail: panospap@ucy.ac.cy

Keywords: CO_2 sequestration, saline aquifer, VOF method, porous media.

Abstract. *In this work we investigate numerically the injection of supercritical carbon dioxide into a deep saline reservoir from a single well. We analyze systematically the sharp-interface evolution in different flow regimes. The flow regimes can be parameterized by two dimensionless numbers, the gravity number, Γ and the mobility ratio, λ. Numerical simulations are performed using the Volume of Fluid (VOF) method and the results are compared with the solutions of the self-similarity equation established in previous works which describes the evolution of the sharp interface. We show that these theoretical solutions are in very good agreement with the results from the numerical simulations presented over the different flow regimes, thereby showing that the theoretical and simulation models predict consistently the spreading and migration of the created CO_2 plume under complex flow behavior in porous media. The present study indicates that the self-similar solutions parameterized by the dimensionless numbers λ, Γ are significant for examining effectively injection scenarios, as these numbers control the shape of the interface and migration of the CO_2 plume. This finding is essential in assessing the storage capacity of saline aquifers.*

1 INTRODUCTION

One of the most popular emerging methods for mitigating the adverse effects of this greenhouse gas is the sequestration (capture and storage) of the carbon dioxide into the subsurface at supercritical conditions [1]. There are many possible geological settings that can be used for this purpose including: depleted oil and gas reservoirs, saline aquifers, coal beds, deep ocean sediments and salt formations [2]. In this work we will examine the saline aquifer as the target formation as it appears to be the most effective possible location for CO_2 storage due to its large potential capacity. The sequestration injection process of carbon dioxide into the subsurface involves nearly immiscible multiphase flow of the supercritical CO_2 and resident fluid. The difference in the densities of the two fluids (CO_2 being less dense and viscous than the resident brine) causes a clear separation with the invading CO_2 layering on the top of the aquifer while the brine host fluid recedes at the bottom of the formation [3]. Furthermore, according to these two fluid properties, the CO_2 can migrate away from the injection site depending on its buoyancy and mobility relatively to the brine. Usually, the modelling of this two-phase flow in porous media involves the complete gravity segregation (sharp interface) approximation and the vertical equilibrium (Dupuit) approximation [3-7] Thus, the problem can be reduced to the determination of the sharp interface evolution. The proper understanding of the interfacial dynamics as encapsulating the displacement process is the focus of many research areas and disciplines related to enhanced oil and coal-bed methane recovery, oil field wastes (mixture of fluids and solvents) from oil production, seawater intrusion, ground water movement, pollutant transport, geothermal reservoirs and environmental assessment and management.

The numerical and analytical modelling of the CO_2 sequestration problem involves many different physical mechanisms. There are three dominant physical processes and trapping mechanisms taking place in both, during and after the injection of CO_2 into geological formations which vary significant with time. First, during and after stopping the injection, advective multi-phase processes dominate when the CO_2 plume is evolving. In this first stage, the multiphase flow is driven by viscous forces due to the injection overpressure and by buoyancy due to the density differences. The time scale associated with this physical process is in the order of a century. After the first phase, the multi-phase flow slows down and the effect of dissolution of CO_2 into the brine increases. The third physical process begins when the time is sufficient to dissolve the injected CO_2 completely or to generate significant mineralization due to geochemical reactions (i.e. precipitation of calcite). The time scales associated with the aforementioned processes are discussed in [8, 9].

The purpose of this work is to investigate the extent at which the self-similar sharp-interface solutions reproduce the behavior of the CO_2 plume as it is captured in the far more detailed modelling by the numerical solutions of a two-phase flow solver. We revisit first the governing equation of the self-similar solutions of the sharp interface equations. This is a non-linear ODE, susceptible only to numerical solution. Due to this necessity the importance of this equation has been somewhat underestimated in the literature. Nonetheless, the self-similarity equation poses a far more tractable problem than dealing with the full two-phase flow under the same conditions. Thus, it can be used as a tool of intermediate difficulty, between the exact analytic expressions on the one hand and full numerical simulations on the other, for making useful predictions about the CO_2 plume evolution under given conditions. Therefore that tool should be assessed regarding the extent to which it reproduces the behavior of the two-phase flow, an undertaking also somewhat neglected in the literature. Thus we compare these solutions against the numerical solutions produced by the volume of fluid method (V.O.F). This comparison is done for a set of cases that essentially cover all the physically different regions in the (Γ,λ) parameter space. Other numerical studies and contributions can be found. in [9]. We find that, at its mature stage and within the period of time where our approximations are physically meaningful, the self-similar solutions capture rather impressively the behavior of the CO_2 plume-brine interface; the fine differences that arise can be classified according to the region in the (Γ,λ) parameter space.

In recent years, researchers have attempted to model the CO_2 sequestration problem assuming axial symmetry to establish fundamental understanding of the process by utilizing both numerical analyses and analytical solutions. The theoretical basis for the basic understanding of the CO_2 plume evolution was presented by [5]. They formulated the advancement of the CO_2 plume in the reservoir as a sharp interface problem under vertical equilibrium using well-known equations in hydrological problems, and presented a self-similarity solution in the regime of fast injection i.e. when buoyancy is virtually negligible. In another important theoretical contribution [3], they managed to derive an expression for the sharp interface evolution through a simplifying interpretation of the Dupuit approximation. The theoretical bounds and the applicability of that solution for predicting the interface is still a matter of discussion by many researchers [3, 7, 10]. In their work they used matching of approximate near-boundary solutions to derive semi-analytic expressions that reproduce quite accurately the self-similarity solutions of the sharp interface equations in the entire (Γ,λ) parameter space, presenting also comparisons with the analytical expressions of [3, 6]. Further analytical studies on the CO_2 sequestration problem have been presented in many other works; see e.g. [11-13].

This work is organized as follows: In section 2, we present the necessary theoretical background as given in the literatura [3, 5, 6]. In section 3, we focus on the description of the numerical models that were created and solved with Ansys-Fluent. The results from the comparisons are presented in section 4.

2 THEORETICAL MODEL

We model the axisymmetric spreading of supercritical CO_2 plume into a porous formation as an immiscible displacement problem; the formation is homogeneous, is confined above and below by impermeable geological settings and is fully saturated by a resident fluid (brine). The problem set up involves a sharp interface between the invading fluid (CO_2) and the resident fluid which are immiscible, assuming vertical equilibrium and neglecting the capillary pressure. In order to minimize complexity the fluids are assumed to be Newtonian, incompressible, and chemically inert.

The validity of the gravity or buoyancy segregation (sharp interface) and vertical equilibrium was discussed by [7], building on the work of [14]. Vertical equilibrium is maintained due to the large aspect ratio of the aquifer i.e. the radial extent of the plume at its mature stage is much larger than the thickness of the aquifer. Indeed, in the case we shall consider the aspect ratio is roughly 100:1 which is more than adequate as the error is of the order $(1/100)^2$. Then, the assumption that the capillarity effects are negligible implies that the fluids are segregated according to density. The assumption that the capillarity effects are negligible is less well founded; indeed, capillary forces may lead to non-negligible transition saturation zone rendering the sharp-interface assumption invalid, or introduce new phenomena which may modify the sharp interface significantly. Nonetheless capillary effects are in general less important than the effects of buoyancy for the problem at hand (see e.g. [11]) and we shall take the capillary pressure as negligible.

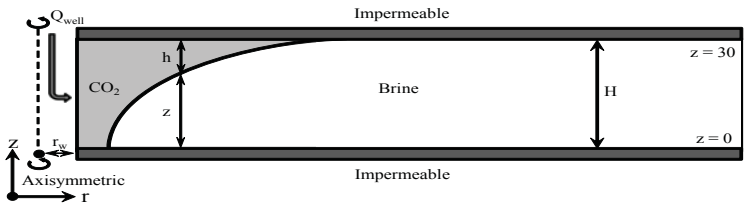

Figure 1. Schematic representation of the problem setting

The injected CO_2 moves radially outward, eventually forming a continuous plume with a well defined borderline (sharp interface) with the resident fluid. Due to the difference in the densities of the resident brine and the CO_2, with the CO_2 being less viscous i.e. more mobile, gravity override will take place directing the injected fluid towards the top of the porous formation (Fig.1). We consider the period during injection. The equations governing the evolution of the interface have been developed by [5,7]; for background theory the reader may consult [4]. We will not add anything new to the derivation of the interface dynamics equations in the problem at hand. We shall therefore simply quote the basic equation from the references. Let k be the intrinsic permeability of the porous medium and ϕ is the porosity of the medium. Let ρ_c, ρ_w be the mass density of the CO_2 and brine respectively, μ_c, μ_w their dynamic viscosities and k_c^r, k_w^r their relative permeabilities. Let $h(r,t)$ be the thickness of the CO_2 plume at time t at distance r from the well. The plume is advancing between the two impermeable layers at $z=0$ and $z=H$. Q is the injection flow rate. The dynamic equation for $h(r,t)$ then reads [2]:

$$\frac{\partial h}{\partial t}=\frac{1}{r}\frac{\partial}{\partial r}\left[\frac{\Delta\rho g k\lambda_w}{\phi}\frac{\lambda h(H-h)}{\lambda h+H-h}r\frac{\partial h}{\partial r}+\frac{Q}{2\pi\phi}\frac{H-h}{\lambda h+H-h}\right] \tag{1}$$

with $\Delta\rho=\rho_w-\rho_c$. The quantities λw, λc are the mobilities of the CO_2 and water, respectively, and λ is the mobility ratio (relative mobility of CO_2) [2]:

$$\lambda=\frac{\lambda_c}{\lambda_w}=\frac{k_c^r/\mu_c}{k_w^r/\mu_w} \tag{2}$$

The mobility ratio λ is the first dimensionless number that makes naturally its appearance and is one of the coordinates of the parameter space in this problem. Equation (1) is by construction consistent with the CO_2 mass conservation [2]:

$$Qt=\phi\pi r_{\text{bed}}^2H+\phi\int_{r_{\text{bed}}}^{r_{\text{cap}}}2\pi rh(r,t)dr=\phi\int_0^H\pi r^2(h,t)dh \tag{3}$$

The distances at which the CO_2 interface meets the bed and the cap of the formation at time t are defined by $h(r_{\text{bed}},t)=H$ and $h(r_{\text{cap}},t)=0$.

The effects of buoyancy are controlled by the first term in the square brackets in (1). The time-scale associated with CO_2 movement due to buoyancy, and therefore associated with the strength of this term in Equation (1), is [2]

$$\tau_{\text{buoyancy}}=\frac{H}{u_{\text{buoyancy}}}=\frac{H\mu_w}{\Delta\rho gk} \tag{4}$$

This scale expresses the time it takes for an injected CO_2 volume to traverse vertically the formation due to buoyancy relatively to the resident fluid. It is formed out of the buoyancy velocity scale which often appears in gravity current analyses (see [15]) and follows directly from Darcy's law. Clearly, the buoyancy time scale is also the time scale of gravity segregation and the formation of a clear interface between the invading and resident fluid.

Consider first the case where buoyancy effects can be neglected. Although buoyancy is initially responsible for the segregation of the two phases it may well become negligible once the sharp interface is formed and (1) holds. One may guess intuitively that, as we shall see explicitly below, this is the case when the scale τbuoyancy is adequately smaller than the injection time scale, Q/H^3. Then Equation (1) becomes a non-linear first order wave equation with spatial variable r^2 [2]:

$$\frac{\partial h}{\partial t}+c(h)\frac{\partial h}{\partial r^2}=0,\qquad c(h)\equiv\frac{Q}{\pi\phi}\frac{\lambda H}{(\lambda h+H-h)^2} \tag{5}$$

The homogeneity of (5) implies that the field h is constant along each characteristic curve. The characteristics therefore read: $r^2=ct+r_0^2$. At times late enough such that the initial condition constant r_0^2 can be dropped, the solution of (5) reads [2]

$$\frac{r^2}{t}=c=\frac{Q}{\pi\phi}\frac{\lambda H}{(\lambda h+H-h)^2} \tag{6}$$

Therefore, Equation (6) is the asymptotic solution of (5) which is the no-buoyancy limit of (1). Clearly, it is also a self-similar solution of (5) i.e. a time-invariant shape for the similarity coordinate r^2/t.

Given Equation (6), the evolution of r_{cap} and r_{bed} follows immediately upon setting $h=0$ and $h=H$ respectively. The vertical average of r^2 reads [2]:

$$\frac{\langle r^2\rangle}{t}=\frac{Q}{\pi\phi H} \tag{7}$$

In fact, Equation (7) is nothing but the volume conservation (equation 3). That is, Equation (7) is a general fact and it holds as long as (1) holds. This result shows that the mean r^2 spreading of the plume interface is determined solely by the invading fluid injection rate Q and the porosity ϕ of the porous medium. The shape of the interface, on the other hand, depends on the mobility of the invading fluid relatively to the resident one as well as on the diffusion effects of buoyancy when the latter is not negligible.

Consider the buoyant self-similar solutions i.e. the self-similar solutions of (1). They are expected to emerge at times at least as large as the buoyancy scale τ_{buoyancy}. Thus we define the dimensionless quantities χ, x by [2]:

$$\frac{r^2}{t}=\frac{Q}{\pi\phi H}\chi, \qquad x=\frac{h}{H} \tag{8}$$

and seek a solution of Equation (1) of the form $h=Hx(\chi)$, where x is the normalized plume thickness: $0\le x\le 1$ and χ is the normalized similarity coordinate chosen so that the volume conservation in (3) translates to [2]:

$$\int_0^1 \chi dx=1 \tag{9}$$

One may observe that the general mean r^2 in (7) follows from Equations (8) and (9). Substituting (8) in (1) yields [2]:

$$-\chi\frac{dx}{d\chi}=\frac{d}{d\chi}\left[2\Gamma\frac{\lambda x(1-x)}{\lambda x+1-x}\chi\frac{dx}{d\chi}+\frac{1-x}{\lambda x+1-x}\right] \tag{10}$$

where Γ is the gravity number [2]:

$$\Gamma=\frac{2\pi H^2\Delta\rho g k\lambda_w}{Q} \tag{11}$$

The gravity number Γ, is the dimensionless parameter encoding the strength of the buoyancy effects as defined by [5]. For $\Gamma=0$ buoyancy is negligible. Equation (10) is the defining equation of the self-similar solutions of (1). The solutions form a two-parameter family of functions depending on the pair (Γ,λ) for $\Gamma\ge 0$ and $\lambda>1$. The gravity number can also be understood as the ratio of the injection to the buoyancy rates (denoted as inverse respective time scales) [2]:

$$\Gamma=2\frac{\tau_{\text{buoyancy}}^{-1}}{\tau_{\text{injection}}^{-1}}, \qquad \tau_{\text{injection}}^{-1}=\frac{Q}{\pi H^3} \tag{12}$$

Equation (12) suggests that if the effects of buoyancy progress fast enough relatively to the injection then the buoyancy effects control the shape the interface appreciably. It is important to note that the buoyancy term i.e. the first term on the right hand side of Equation (1) expresses diffusion of the CO_2 mass in the radial direction. The gravity number Γ can be seen as the relative strength of that term in the equation. That is, when the gravity number is large we have a relatively strong diffusion of the CO_2 plume outwards. Finally, we notice that the gravity number Γ does not depend on the mobility of the invading fluid. Therefore, Γ and λ are indeed independent parameters.

It is more convenient to try to determine the functions $\chi(x)$ i.e. to solve for the distance r as a function of the plume thickness h, and not the other way around. After all the range of values of the normalized thickness x is fixed, $0\le x\le 1$, while the range of values of r and therefore of χ is part of the solution. Let us define the volume function [2]:

$$\psi(x)=\int_x^1 \chi(x')dx' \tag{13}$$

This is the volume of the CO_2 from the bed of the formation ($x = 1$) to thickness x . Clearly, if $\psi(x)$ is known then $\chi(x)$ is also known [2]:

$$\chi(x) = -\psi'(x) \tag{14}$$

where the prime denotes differentiation. Integrating, Equation (10) becomes [2]

$$\psi = \psi_0 \left(1 + 2\Gamma\lambda\, x \frac{\psi'}{\psi''} \right), \qquad \psi_0 = \frac{1-x}{1+(\lambda-1)x} \tag{15}$$

where ψ_0 is the no-buoyancy ($\Gamma = 0$) volume function, as it follows clearly from (15) in a trivial algebraic way. By Equation (14), the solution ψ_0 gives the no-buoyancy solution [2, 5]:

$$\chi = \frac{\lambda}{(1+(\lambda-1)x)^2} \tag{16}$$

which also follows algebraically from the self-similarity Equation (10) for Γ=0. In other words, the result in (16) is the solution of (6) that is obtained explicitly above as an asymptotic solution of (1) in the limit of negligible buoyancy.

Implicit in the derivation of Equation (15) from (10) is the volume conservation of (6) that is encoded in (10). Therefore, as one may verify directly, it need not be used as an independent condition. In other words, Equation (10) is equivalent to (15) together with the end-point conditions:

$$\psi(0) = 1, \qquad \psi(1) = 0 \tag{17}$$

The first condition expresses the mass conservation, followed by Equation (9) and the definition of (13), while the second is a mere implication of the definition. Equation (15) and the conditions (17) define completely the mathematical problem at hand. This problem must be solved numerically. The result is a specific curve ψ(x) of each pair (Γ, λ). Through (13) and the definitions of (8) this curve translates to the evolving interface curve of all two-phase flows characterized by the pair (Γ, λ).

3 NUMERICAL MODELLING

The modelling of CO_2 injection as an immiscible displacement problem possesses special challenges because of the nonlinearities inherent in the multiphase flow regimes and their interaction with the porous formation. As closed form analytical solutions are rare and apply under special conditions, numerical simulations provide valuable tools to investigate the dynamics of the CO_2 front invading the porous medium.

The PISO is an efficient method to solve the Navier-Stokes equations in unsteady and in severely nonlinear problems. The main advantages of this method are a) no under-relaxation is applied and b) the momentum corrector step is performed more than once. The algorithm can be summarized as follows: 1) set the boundary conditions, 2) solve the discretized momentum equations to compute an intermediate velocity field, 3) compute the mass fluxes at the cells faces, 4) solve the pressure equation, 5) correct the mass fluxes at the cell faces, 6) correct the velocities on the basis of the new pressure field, 7) update the boundary conditions (if required from the problem at hand), 8) repeat from step (3) for a prescribed number of times, 9) increase the time step and repeat from step (1). Steps (4) and (5) are repeated for a prescribed number of times to correct for non-orthogonality of the control volumes in the numerical solution [2].

The discretized domain was considered to be 5000 m $\times$ 30 m (Fig. 1) to ensure vertical equilibrium in the numerical solution. The wellbore location is at the left corner. In the geometric construction of the model we have also considered the wellbore radius rw = 0.15 m. For a long formation (i.e. 5 km) the size of the wellbore radius is negligible and its effects in the evolution of the CO_2 plume can be ignored. The model is axisymmetric by construction. The CO_2 is injected along the wellbore as an inlet boundary condition. No flow conditions (walls) were imposed at the bottom and at the top side of the models. These conditions are true for an aquifer with impermeable upper and lower boundaries (i.e. confined). At the right end of the models outlet boundary conditions were used with zero gauge pressure to ensure the flow path. The changes that are expected between the interface of the two fluids and the strong interaction of the multiphase flow in the porous formation with the cap rock, is dealt with placing a sufficient fine mesh around the wellbore and in the vicinity of the caprock.

The calculations were carried out in Ansys-Fluent, a nonlinear finite volume code suit of programs. The usual 8-node tetrahedral cell elements were used to model the fluid flow in the aquifer and the interface evolution process. The computation of the fluid diffusion in the porous domain and the interface evolution process is performed by the displacement of the dense fluid (brine) by the less dense (CO_2) in the cells center [2].

4 RESULTS

In this section we present the results from the multiphase flow analysis that has been conducted for the modeling of the spreading of supercritical CO_2 plume into a porous formation. As already mentioned, the analysis classifies all cases of plume interface evolution according to the pair of dimensionless numbers (λ, Γ). In order to get a feeling of the physically interesting values, first of all we note that according to [6] the cases of practical interest can be classified into shallow and deep aquifer formations and further into warm and cold formations. In these categories the mobility ratio varies as: a) shallow-warm: $21.3<\lambda<38.4$, b) shallow-cold: $13.8<\lambda<27.4$, c) deep-warm: $4.9<\lambda<7.9$ and d) deep-cold: $6.2<\lambda<10.5$. The aforementioned range of the mobility ratios suggests that the injected fluid is more mobile than the ambient fluid in the formation. In general, the CO_2 being less mobile than the resident fluid is highly rare to occur in saline aquifer formations. Thus we shall restrict ourselves to the cases where $\lambda>1$, considering values also near to the borderline value $\lambda=1$ as they exhibit their own interesting behavior. At the other end of the range of λ, it turns out that it is adequate to consider values of λ at most up to 30, as these cases essentially exhaust the qualitatively different types and behavior of the plume interface as that is compared to the associated self-similar solution. For the gravity number we shall consider the range $0.2 \leq \Gamma \leq 15$. This covers the range of reasonable injection scenarios as well as the range of cases that exhibit qualitative distinct and interesting behavior.

The input parameters upon which the numerical computations were performed are given in Table 1. These parameters include the geometric properties of the wellbore and the formation, the porous rock formations properties, the fluids properties and the pumping parameters. Furthermore, we also show the variance of the mobility ratio, λ according to the fluid properties and the variance of the gravity number, Γ according to the pumping parameters. The mobility ratio is calculated from equation (2) while the gravity number from equation (11).

Variable					**Value**
Geometric properties					
Aquifer thickness, **H [m]**					30
Wellbore radius, $\mathbf{r_w}$ **[m]**					0.15
Wellbore face area, **A [m^2]**					28.35
Porous formation properties					
Rock permeability, **K [m^2]**					2E-14
Porosity, **φ [-]**					0.15
Fluids properties					
Water density, **ρw [kg/m^3]**					1045
Water viscosity, μ_w **[kg/sec.m]**					2.54E-4
CO_2 density, ρ_c **[kg/m3]**					479
CO_2 viscosity, μ_c **[kg/sec.m]**	2.54E-4	2.12E-4	4.23E-5	1.69E-5	8.47E-6
Mobility ratio, **λ [-]**	1	1.2	6	15	30
Pumping parameters					
Superficial velocity, **u [m/sec]**	4.36E-4	8.72E-5	1.74E-5	5.81E-6	
Injection flow rate, **Q [m^3/sec]**	1.24E-2	2.47E-3	4.93E-4	1.65E-4	
Gravity number, **Γ [-]**	0.2	1	5	15	

Table 1 : Model input data [2]

In order to investigate the influence of the interface, we have performed a number of parametric studies that will be described in the following. These studies include a) the influence of the mobility ratio, λ (low to high mobility) and b) the influence of the gravity number, Γ (from fast for no-buoyancy to slow with buoyancy).We compare the results of the full numerical solutions with the numerical solutions of the self-similar equation (10). Figures (2) to (5) show two curves that correspond to the full numerical simulation and the numerical solution of the self-similar equation (10). The Y-axis is the interface height normalized with the aquifer thickness i.e. it is the variable we have denoted x. The x-axis is the distance of the interface normalized with the scaling adopted from [6]. The normalized distance equals $\sqrt{\chi}$ where χ is the variable defined in equation (8). Presumably, equation (7) implies that the normalizing factor, that involves $\sqrt{t}$, is nothing but the vertical mean of the aquifer distance from the well. All results presented illustrate the interface at the mature state of evolution. For the choice of parameters of Table 1, the buoyancy time-scale defined in equation (4) is 2.2 years. The full numerical solution results show a number of plume interfaces that correspond to different times frames that range from a few to nearly a hundred buoyancy time-scales. We observe that the expected $\sqrt{t}$ scaling of the plume advancement, encoded in the normalized distance $\sqrt{\chi}$ from the aquifer, is indeed very nicely respected.

We organize the results in sets of graphs with each set corresponding to fixed CO_2 relative mobility λ and

increasing gravity number Γ=0.2, 1, 5, 15. Figure (2) corresponds to λ=1. As in this case the CO_2 is not very mobile, it takes a very large gravity number i.e., an injection rate which is weak relatively to the rate of the buoyancy effects, for the plume to diffuse substantially outwards while moving upwards. With decreasing gravity number the shape of the interface approaches the essentially vertical ('plug flow') form, as predicted by the exact no-buoyancy solution (16) in the limit of λ approaching 1. For all the range of Γ, the full numerical solution and the numerical solution of the self-similar equation (15) are still in a very good agreement.

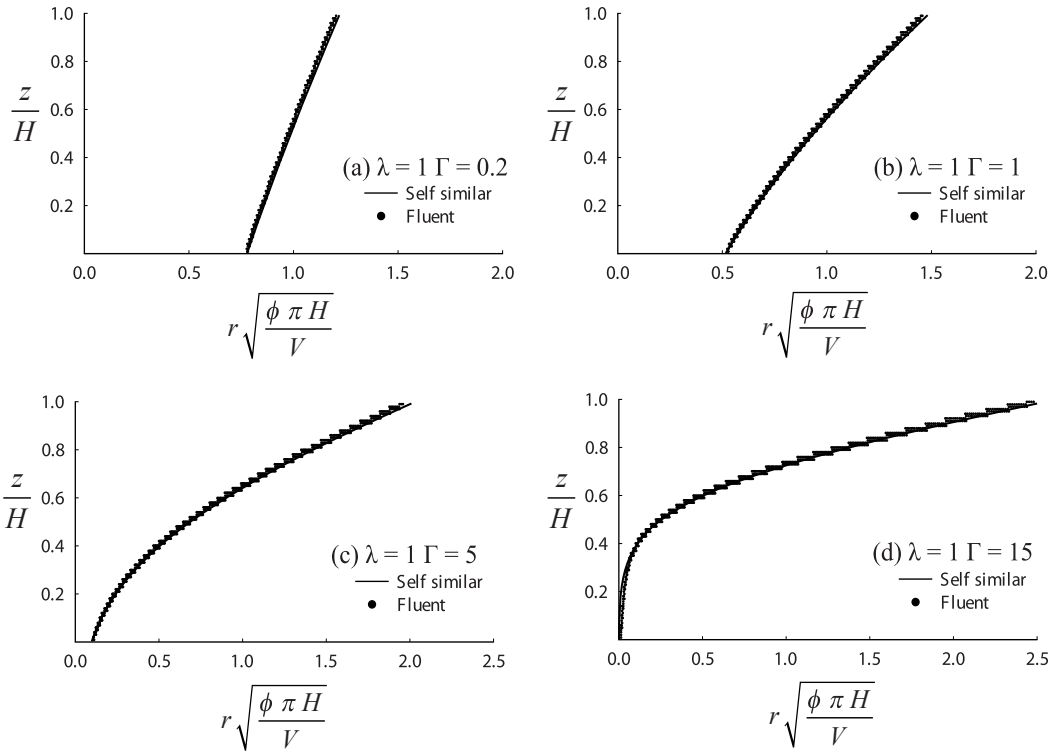

Figure 2. Comparisons of Interface evolution for λ =1 and Γ: 0.2, 1, 5, 15

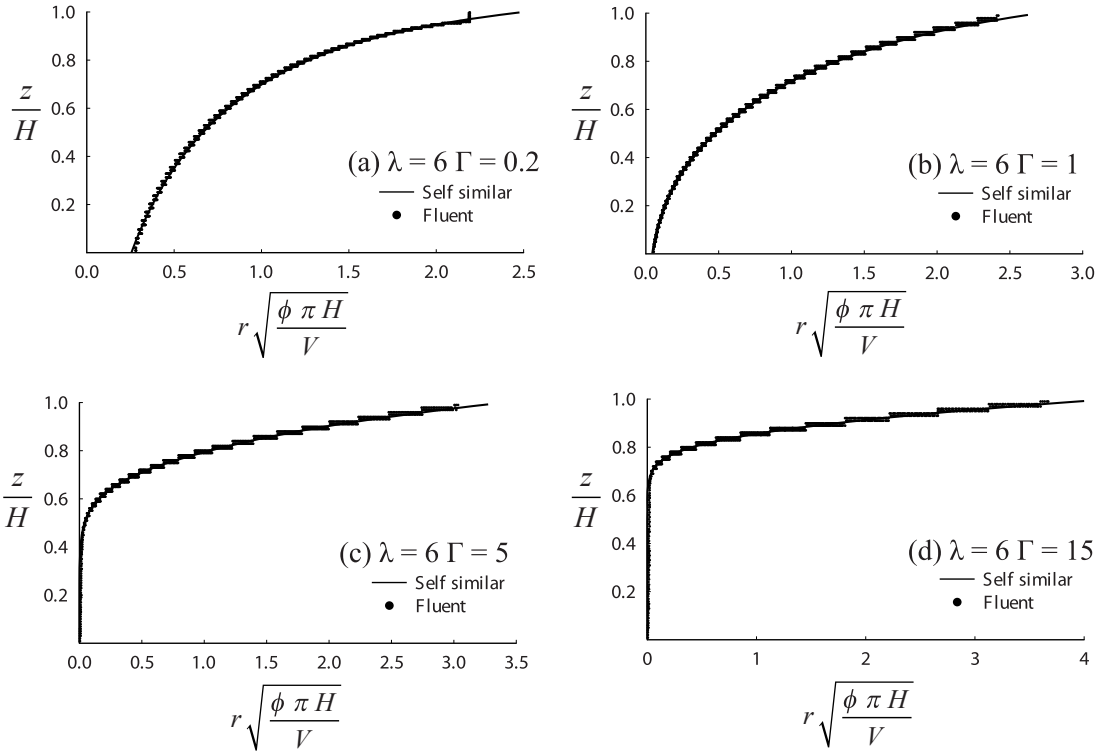

Figure 3. Comparisons of Interface evolution for λ =6 and Γ: 0.2, 1, 5, 15

The second set of results, presented in Fig. 3, corresponds to CO_2 relative mobility ratio λ=6. Here the more

mobile CO_2 plume directs itself substantially outwards and upwards for smaller gravity numbers. The set of graphs shown in Fig. 4 corresponds to CO_2 relative mobility ratio, λ=15. The strongly mobile CO_2 plume directs itself quite well upwards even for relatively weak buoyancy, as shown already from the first graph that corresponds to Γ=0.2. The interface is already quite convex with its tail quite close to the well. The agreement of the simulation results with the associated self-similarity solution is again very good but a subtler effect of the stronger CO_2 mobility makes its appearance.

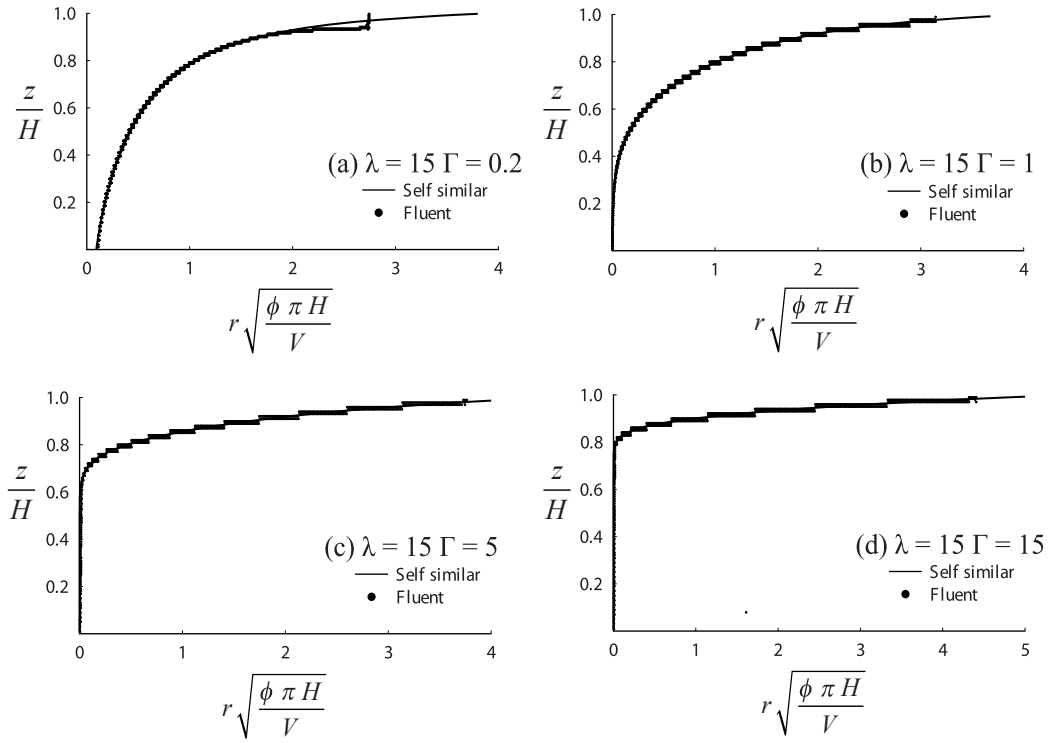

Figure 4. Comparisons of Interface evolution for λ =15 and Γ: 0.2, 1, 5, 15

Already in the λ=6 cases we may observe that the simulations are in very good agreement with the numerical solution of Equation (15) except in the case of Γ=0.2. The small discrepancy observed is by no means a numerical artifact or instability. We see that the stronger CO_2 mobility together with the relatively weak buoyancy forces the top of the interface to deform by accumulation of excessive CO_2 mass that is driven outwards but not strongly enough upwards. This effect is amplified in the λ=15 set of cases. We may explain this phenomenon somewhat better as follows. As mentioned in section 2, mobility and injection alone operate essentially through wave propagation in this problem while, on the other hand, buoyancy introduces explicitly diffusion in the radial direction through the second derivative term in (1). The dynamics of the full two-phase flow appears to works more or less on a similar basis, this is why the self-similar solutions deviate slightly from the full numerical solutions. We suggest that, regarding the cases presented in Fig. 4, the strongly mobile CO_2 fluid advances faster than it can diffuse, thus accumulating at the top of the formation. The relaxation time of this phenomenon, i.e. the time it takes the CO_2 mass to diffuse and form a smooth interface according to self-similarity, should be larger than the $\tau_{buoyancy}$ by a factor in the order of the aspect ratio of CO_2 plume at the mature stages of its evolution. Indeed the full numerical solutions show that the phenomenon diminishes slowly with time.

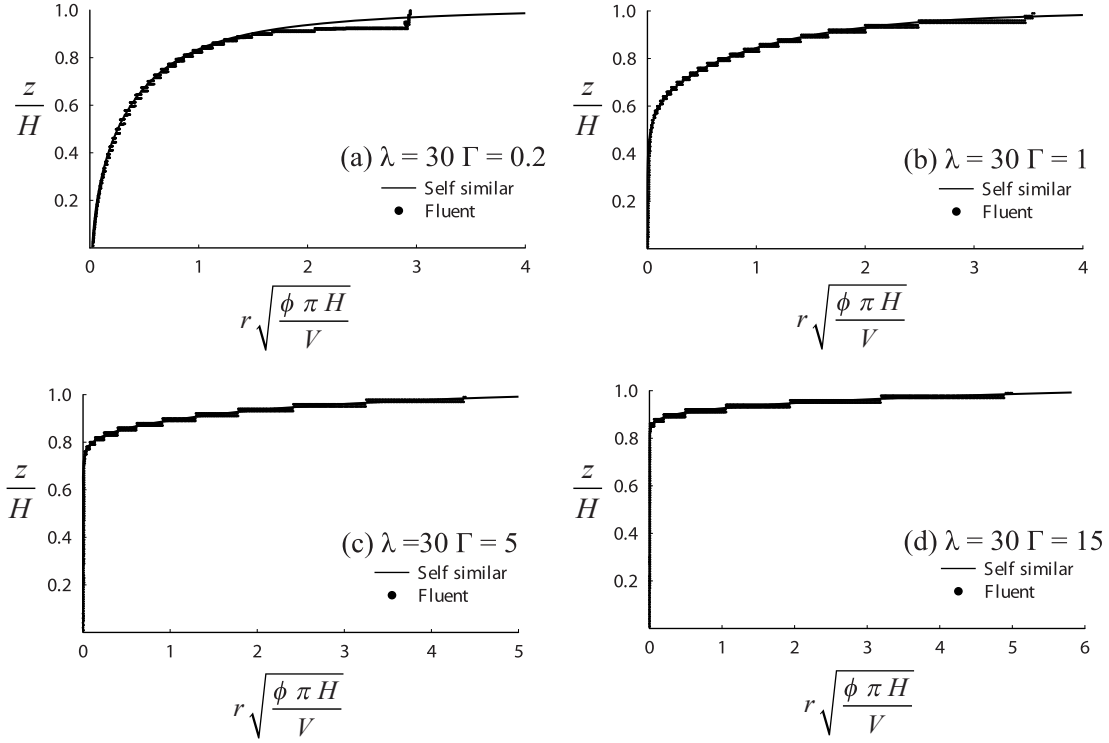

Figure 5. Comparisons of Interface evolution for λ =30 and Γ: 0.2, 1, 5, 15

The final set of results is presented in Fig. 5 and correspond to CO_2 relative mobility ratio λ=30. Here one observes the effects of a highly mobile CO_2 amplified further. Much weaker buoyancy is required to direct the CO_2 mass upwards and to bend the interface to any fixed degree. The weak buoyancy cannot diffuse the CO_2 masses that advance also outwards with even greater ease, leading to greater CO_2 mass accumulation at the top part of the interface.

5 CONCLUSIONS

We have considered the axisymmetric advancement of CO_2 plume, injected in a fully saturated confined saline aquifer. From the detailed numerical investigation conducted we reach the following general conclusions:

The full numerical solutions obtained with Ansys-Fluent showed an overall excellent agreement with the numerical solutions of the self-similar equation (10) or (15) over the entire relevant part of the gravity and mobility (Γ, λ) parameter space i.e. a part where the two-phase flow interface exhibits qualitatively distinct behavior that allows one to perform meaningful comparisons. Other research works which have presented similar comparisons have been rather less detailed [6, 16].

The region of the parameter space where discrepancies arise between the full numerical solutions and the associated exact self-similar solutions is the region of small Γ i.e. when the rate of the buoyancy effects is smaller than the rate of injection, and large CO_2 relative mobility λ i.e. for a highly mobile CO_2 plume through the resident brine. In these cases an amount of CO_2 mass tends to accumulate at the top part of the interface. The reason is that the highly mobile CO_2 directs itself with ease both upwards and outwards while the relatively weak buoyancy, which mathematically operates as radial diffusion, cannot disperse the CO_2 mass accumulated at the top part of the interface. Indeed, according to Equation (1), the more mobile invading fluid is going to move upwards even for literally zero gravity. When buoyancy is not weak the mentioned diffusion effects is what gives the interface the shape predicted by the exact-self similar solutions. The CO_2 mass accumulation at the top of the interface is also visible in other research works [6, 16] but the reasons and the conditions of its occurrence have not been discussed.

ACKNOWLEDGEMENTS

This work was co-funded by the European Regional Development Fund and the Republic of Cyprus through the Research Promotion Foundation (Project: DIDAKTOR/0311/58).

REFERENCES

[1] Bachu, S. (2003), "Screening and ranking of sedimentary basins for sequestration of CO_2 in geological media in response to climate change", *Environmental Geology*, Vol. 44(3), pp. 277-289.

[2] Sarris, E., Gravanis, E. and Papanastasiou P. (2014), "Investigation of the self-similar interface evolution in carbon dioxide sequestration in saline aquifers", *Transport in Porous Media*, DOI: 10.1007/s11242-014-0304-9.

[3] Dentz, M. and Tartakovsky, D. (2009), "Abrupt-interface solution for carbon dioxide injection into porous media", *Transport in Porous Media*, Vol. 79, pp.15-27.

[4] Bear, J. (1972), *Dynamics of Fluids in Porous Media*. American Elsevier Inc., New York.

[5] Nordbotten, J.M. and Celia, M. A. (2006), "Similarity solutions for fluid injection into confined aquifers", *Journal of Fluid Mechanics*, Vol. 561, pp. 307-327.

[6] Nordbotten, J.M., Celia, M.A. and Bachu, S. (2012), "Injection and storage of CO_2 in deep saline aquifers: analytical solution for CO_2 plume evolution during injection", *Transport in Porous Media*, Vol. 58(3), pp. 339-360.

[7] Houseworth, J.E. (2012), "Matched boundary extrapolation solutions for CO_2 well-injection into saline aquifer", *Transport in Porous Media*, Vol. 91, pp. 813-831.

[8] IPCC (2005), *Special report on carbon dioxide capture and storage*, Technical report, intergovernmental panel on climate change (IPCC), prepared by working group III, Cambridge University Press, Cambridge.

[9] Class, H., Ebigbo, A., Helmig, R., Dahle, H.K., Nordbotten, J.M., Celia, M.A.,Audigane, P., Darcis,M., Ennis-King, J., Fan, Y.Q., Flemisch, B., Gasda, S.E., Jin, M., Krug, S., Labregere, D., Beni, A.N., Pawar, R.J., Sbai, A., Thomas, S.G., Trenty, L. and Wei, L.L. (2009), "A benchmark study on problems related to CO_2 storage in geologic formations", *Computational Geosciences*, Vol. 13(4), pp. 409–434.

[10] Lu, C., Lee, S.Y., Han, W.S., McPherson, B.J. and Lichtner, P.C. (2009), "Comments on Abrupt-interface solution for carbon dioxide injection into porous media", by M. Dentz and D. Tartakovsky, *Transport in Porous Media*, Vol. 79, pp. 29-37.

[11] MacMinn, C.W. and Juanes, R. (2009), "A mathematical model of the footprint of the CO_2 plume during and after injection in deep saline aquifer systems", *Energy Procedia*, Vol. 1(1), pp. 3429-3436.

[12] Hesse, M.A., Tchelepi, H.A., Cantwell, B.J. and Orr, F.M. (2007), "Gravity currents in horizontal porous layers: transition from early to late self-similarity", *Journal of Fluid Mechanics*, Vol. 577, pp. 363-383.

[13] Wang, L., Liu, Y. and Chu, K. (2012), "A simplified model and similarity solutions for interfacial evolution of two-phase flow in porous media", *Transport in Porous Media*, Vol. 93, pp. 721-735.

[14] Yortsos, Y.C. (1995), "A theoretical analysis of vertical flow equilibrium", *Transport in Porous Media*, Vol. 18, pp. 107-129.

[15] Huppert, H.E. and Woods, A.W. (1995), "Gravity driven flows in porous layers", *Journal of Fluid Mechanics*, Vol. 292, pp. 55-69.

[16] Liu, Y., Wang, L. and Yu,B. (2010), "Sharp front capturing method for Carbon dioxide plume propagation during injection into deep confined aquifer", *Energy Fuels*, Vol. 24, pp. 1431-1440.